MATHEMATICS OF COMPUTATION
S 0025-5718(09)02188-7
Article electronically published on January 6, 2009

SOLUTION OF $F(z+1)=\exp\big(F(z)\big)$ IN COMPLEX z-PLANE

DMITRII KOUZNETSOV

ABSTRACT. Tetration F as the analytic solution of equations $F(z-1)=\ln(F(z))$, $F(0)=1$ is considered. The representation is suggested through the integral equation for values of F at the imaginary axis. Numerical analysis of this equation is described. The straightforward iteration converges within tens of cycles; with double precision arithmetics, the residual of order of 1.e-14 is achieved. The numerical solution for F remains finite at the imaginary axis, approaching fixed points L, L^* of logarithm ($L=\ln L$). Robustness of the convergence and smallness of the residual indicate the existence of unique tetration $F(z)$, that grows along the real axis and approaches L along the imaginary axis, being analytic in the whole complex z-plane except for singularities at integer the $z<-1$ and the cut at $z<-2$. Application of the same method for other cases of the Abel equation is discussed.

1. INTRODUCTION

The practical ability to deal with big numbers depends on their representation. The positional numeral system has allowed us to write most of the required numbers throughout the centuries. Invention of the floating point enabled huge numbers, although the "floating overflow" still occurs, if the logarithm of a number happens to be too large. The range of huge numbers, distinguishable from infinity in computational mathematics, can be drastically extended, using a function with fast growth [1], for example, the Ackermann functions [2]. Perhaps, the fourth of the Ackermann functions provides fast enough growth for the needs of this century. The function $A(4,x)$ can be expressed in the form

$$A(4,z) \;=\; \underbrace{2^{2^{\cdot^{\cdot^{\cdot^{2}}}}}}_{z-3 \text{ times}} \;-\;3 \;=\; {\exp_2}^{z-3}(1)-3, \tag{1.1}$$

where

$${\exp_a}^{z}(t) \;=\; \underbrace{\exp_a\Big(\exp_a\big(\ldots\exp_a(t)\ldots\big)\Big)}_{z \text{ exponentials}}, \tag{1.2}$$

means application of the exponential z times. Various names are used for the this operation: "generalized exponential function"[1], "ultraexponentiation"[3], "superexponentiation" [4], "tetration"[5]. I use the shortest one, "tetration". This name indicates that this operation is forth in the hierarchy of operations, after summation, multiplication and exponentiation. For the first three operations, the analytic

Received by the editor March 17, 2008 and, in revised form, June 20, 2008.
2000 *Mathematics Subject Classification.* Primary 30A99; Secondary 33F99.

extension for the complex values of the argument is established; and these operations are recognized as elementary functions [6, 7]. Tetration is not yet considered as a special function; the extension for real and complex values is not yet established; iteration of a transcendental function of a complex variable is not trivial [8, 9, 10].

The tetration (1.2) can be written as the recurrent equation

$$\exp_a^z(t) = \exp_a\bigl(\exp_a^{z-1}(t)\bigr);\ \exp_a^0(t) = t, \tag{1.3}$$

for the integer $z > -2$. In this paper, I consider only the case $t{=}1$, $a{=}\mathrm{e}{=}\exp(1)$. In order not to write the main argument z as a superscript, let $F(z) = \exp_{\mathrm{e}}^z(1)$; then, for F I have the equation

$$F(z+1) = \exp\bigl(F(z)\bigr), \tag{1.4}$$

mentioned in the title. Together with the condition

$$F(0) = 1, \tag{1.5}$$

equation (1.4) can be considered as the definition of tetration of an integer argument, larger than -2; it is a special case of equation (1.2) at $a = \mathrm{e}$ and $t = 1$. Such a tetration, as well as the Ackermann functions [2], could be used as a rapidly growing function to represent huge numbers in computers.

Equation (1.4), even together with condition (1.5), does not define an unambiguous function; for additional requirements, assumptions are necessary to specify it. Such an assumption could be that $F'(z)$ is a continuous nondecreasing function in the range $z > -1$. This leads [3] to the piecewise uxp, which can be defined in the following way:

$$\mathrm{uxp}(z) = \begin{cases} \ln\bigl(\mathrm{uxp}(z{+}1)\bigr) & \text{at} \quad \Re(z) \le -1, \\ z+1 & \text{at} \quad -1 < \Re(z) \le 0, \\ \exp\bigl(\mathrm{uxp}(z{-}1)\bigr) & \text{at} \quad 0 < \Re(z). \end{cases} \tag{1.6}$$

This function is shown in the top of the Figure 1(a); lines of constant amplitude and constant phase are drawn. Discontinuities (cuts) are marked with thick lines. At the real axis, function uxp has continuous derivative; it is analytic in the complex z-plane with cuts at $z \le -2$ and at $\Re(z) \in$ integers. These cuts separate the complex plane to almost independent segments. The figure raises questions of whether all of these cuts are necessary, or if some solutions of equation (1.4) are more regular. As a sketch of such a solution, in Figure 1(b), I also plot the function

$$\mathrm{Fit}_3(z) = \begin{cases} \ln\bigl(\mathrm{Fit}_3(z{+}1)\bigr) & \text{at} \quad \Re(z) \le -1, \\ \mathrm{fit}_3(z) & \text{at} \quad -1 < \Re(z) \le 0, \\ \exp\bigl(\mathrm{Fit}_3(z{-}1)\bigr) & \text{at} \quad 0 < \Re(z), \end{cases} \tag{1.7}$$

where

$$\mathrm{fit}_3(z) = 0.6\ \mathrm{fit}_2(z) + 0.4\ \ln\bigl(\mathrm{fit}_2(z+1)\bigr), \tag{1.8}$$

$$\mathrm{fit}_2(z) = \ln(2{+}z) + (1{+}z)\left(1 + \frac{z}{2}\exp\Bigl((z{-}1)s_2(z)\Bigr)\Bigl(\mathrm{e}{-}2{+}\ln\frac{4}{3}\Bigr) - \ln 2\right), \tag{1.9}$$

$$s_2(z) = \exp\Bigl(\exp(z-2.51)\Bigr) - 0.6 + 0.08(z{+}1). \tag{1.10}$$

Function Fit_3 has the same cuts of the range of analyticity, as function uxp, but in the range of Figures 1(a,b), the jumps are small and are not seen.

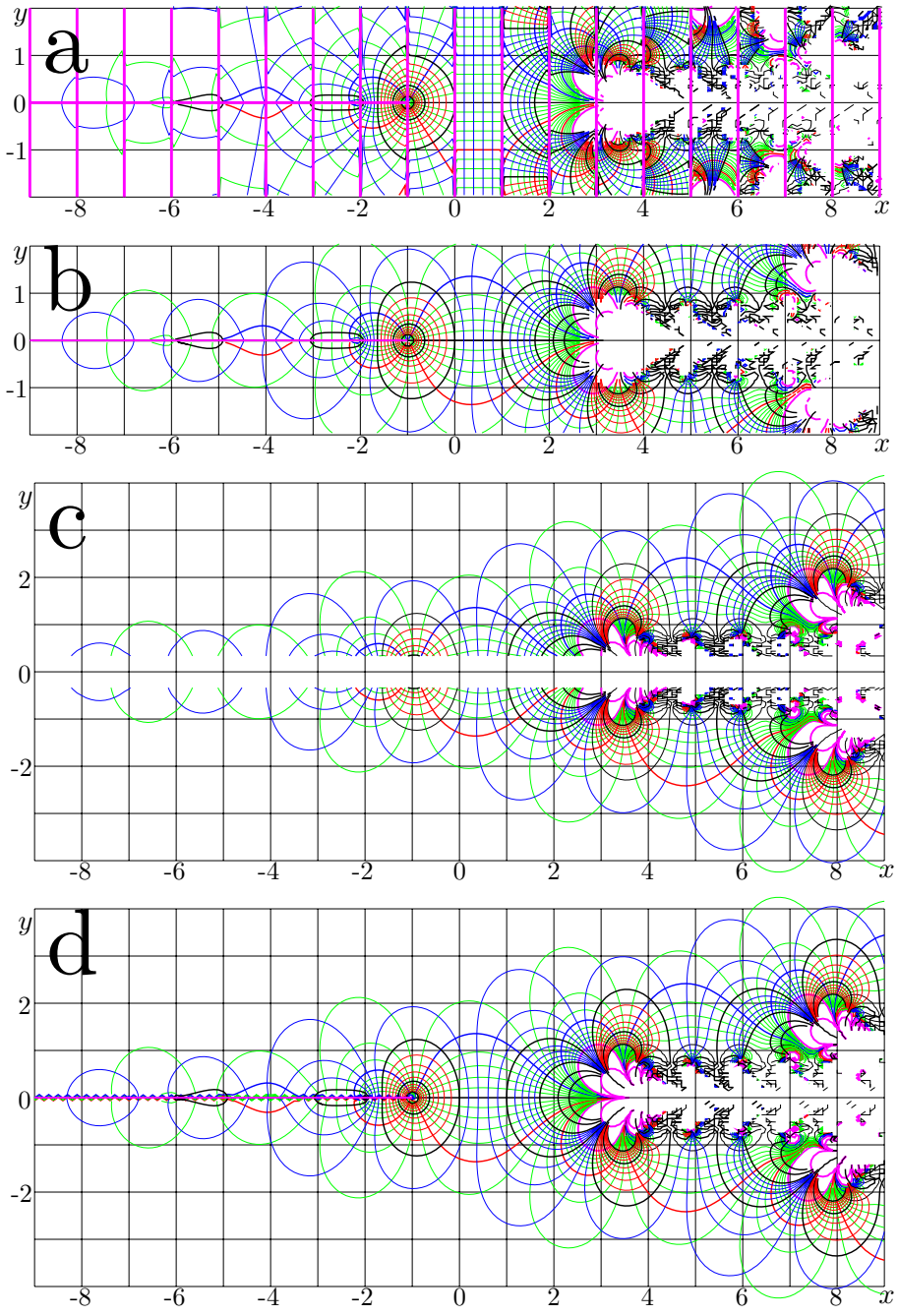

FIGURE 1. (a) Function $f = \mathrm{uxp}(x+\mathrm{i}y)$ by equation (1.6) at the complex plane. Levels $|f| = 1$, $\exp(\pm1)$, $\exp(\pm2)$, $\exp(\pm3)$, $\exp(\pm4)$ and $\arg(f) = 0$, ±1, ±2, ±3 are shown with thick lines. (b)–(d) the same for functions Fit_3 by equation (1.7), Fit_4 by equation (2.16), and solution F by (5.5).

In the following, I *assume* that there exists unique analytic tetration F, which has properties, similar to those of the function Fit_3, seen in Figure 1(b); then I guess the asymptotic behavior of function F, which allows one to plot part (c) of the figure. I collect such guesses and assumptions in Section 2.

In Section 3, I interpret the asymptotic fit in terms of the entire solution of (1.4).

In Section 4, I express the analytic tetration with the contour integral, which leads to the integral equation (4.5) for values of tetration at the imaginary axis.

In Section 5, I describe the numerical (iterational) solution of this integral equation, which allows one to evaluate function F and plot Figure 1(d).

In Section 6, I estimate the precision of the numerical solution and provide tables of its values at the imaginary axis and those at the real axis.

In Section 7, I discuss properties of the inverse function.

In Section 8, I compare the values of the analytic tetration with other solutions of equation (1.4) at the real axis.

In Section 9, I suggest possible application of the formalism to the fiber optics.

In Section 10, I discuss the generalization for other cases of the Abel equation and complex Ackermann functions.

In Section 11, I formulate the theorem pertaining to existence and uniqueness of analytic tetration and request for the mathematical proof.

2. Assumptions

In this section I discuss properties of the function Fit_3, seen in Figure 1, and postulate them as assumptions, as requirements for the analytic tetration $F(z)$.

The equation (1.4) could allow more solutions than equation

$$\ln(F(z+1)) = F(z)\ . \tag{2.1}$$

In this paper I assume that the logarithm ln is a single-valued function, that is, analytic at the complex plane with the cut along the negative part of the real axis. Then, all the solutions of equation (2.1) are solutions of (1.4), but it is not obvious that a solution F of (1.4) also satisfies (2.1). One could add term $2\pi\mathrm{i}$ to the right hand side of equation (2.1), and the solution of the resulting equation will also be the solution of (1.4). In searching for the simple tetration, I begin with analytic solutions, which also satisfy equation (2.1).

Assumption 0. The analytic solution $F(z)$ of equation (2.1) exists in the whole complex z-plane, except for part of the real axis $z \le -2$; this solution satisfies $F(z^*) = F(z)^*$, and $F(0)=1$.

From Assumption 0 it follows that $F(z)$ is real at real $z > -2$. As the argument z emerges from the real axis, the approximation $\mathrm{Fit}_3(z)$ approaches (although it does not reach this asymptotic exactly within the range of approximation) the fixed points L and L^* of the logarithm, which are solutions of the equation

$$L = \ln(L). \tag{2.2}$$

The graphic (computational) search for the solution of equation (2.2) is shown in Figure 2(a). Fixed points of the logarithm should not be confused with fixed points of the exponential, shown in Figure 2(b); fixed points of exponentials are solutions of equation

$$L = \ln(L) + 2\pi\mathrm{i}\ m \tag{2.3}$$

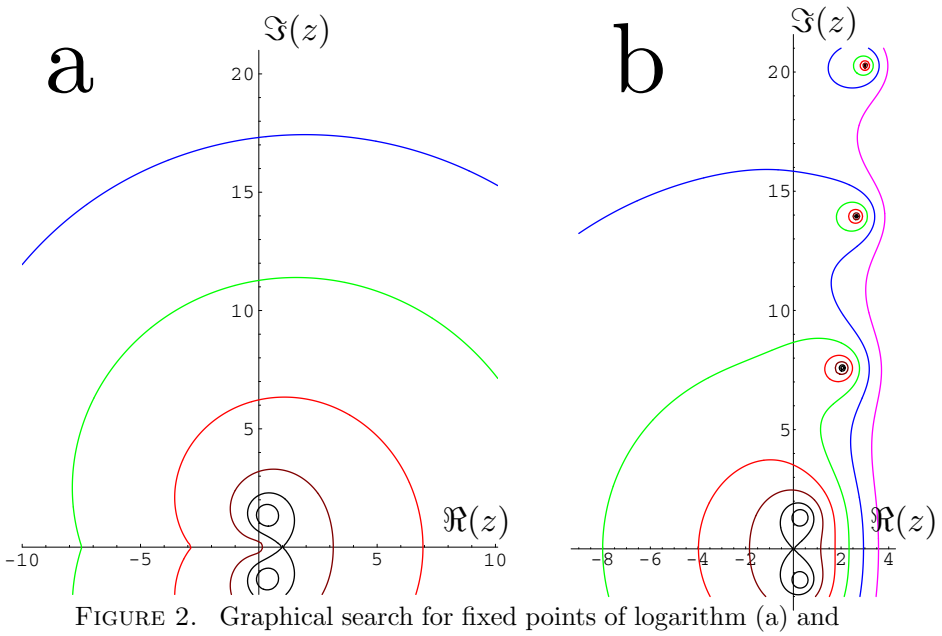

FIGURE 2. Graphical search for fixed points of logarithm (a) and for the exponential (b). Functions $f=|\ln(z)-z|$ and $f=|\exp(z)-z|$ are shown with levels $f=1/4$, $f=1/2$, $f=1$, $f=2$, $f=4$, $f=8$, $f=16$ in the complex z-plane.

for integer values of m. All fixed points of the logarithm are fixed points of the exponential, but only two of the fixed points of the exponential are fixed points of the logarithm, and only one of them is in the upper half-plane. The straightforward iteration of equation (2.2) converges within a hundred evaluations, giving the approximation

$$L \approx 0.31813150520476413 + 1.3372357014306895\,\mathrm{i}\,. \tag{2.4}$$

More rigorous analysis of the fixed points of the exponential (Ruhewerte der Exponentialfunktion) can be found in [11].

Let the analytic tetration F approach values L and L^* at $\pm\mathrm{i}\infty$:

Assumption 1. Tetration F satisfies the relation

$$\lim_{y\to+\infty} F(x+\mathrm{i}y) = L \quad \text{for all real} \quad x\,. \tag{2.5}$$

From Assumption 0, it follows that

$$\lim_{y\to-\infty} F(x+\mathrm{i}y) = L^* \quad \text{for all real} \quad x\,. \tag{2.6}$$

The imaginary part of Fit_3 becomes positive at positive values of the imaginary part of the argument; this corresponds to positive values of the derivative of tetration at the real axis. For initial value with positive real part and positive imaginary part, the iteration of equation (2.2) converges to L. Within the range of Figure 1(b), function $\mathrm{Fit}_3(z)$ approaches L at negative $\Re(z)$ and positive $\Im(z)$, and $\mathrm{Fit}_3(z)$ approaches L^* at negative $\Re(z)$ and negative $\Im(z)$. Due to convergence of the iterative solution of equation (2.2), the analytic tetration F should keep the asymptotic

(2.5) at any fixed value of the imaginary part of the argument:

$$\begin{array}{lll} \lim\limits_{x\to-\infty} F(x+\mathrm{i}y) = L & \text{at} & y>0, \\ \lim\limits_{x\to-\infty} F(x+\mathrm{i}y) = L^* & \text{at} & y<0. \end{array} \tag{2.7}$$

The iteration of the logarithm leads to the exponentially convergent sequence. Let the function $F(x+\mathrm{i}y)$ at $x\to-\infty$ approach its limiting value, also exponentially:

$$F(z) = L + \varepsilon(z) + o(\varepsilon(z)) \ , \tag{2.8}$$

where

$$\varepsilon = \exp(Qz+r), \tag{2.9}$$

Q and r are complex constants, $\Re(Q)>0, \Im(Q)>0$.

The substitution of equation (2.8) to equation (1.4) gives $Q=L$. The constant

$$T = 2\pi/L \approx 1.05793999115694 - 4.44695072006701\mathrm{i}, \tag{2.10}$$

is quasi-period: for moderate values of $\Re(z)$,

$$F(z+T) \approx F(z) \quad \text{at} \quad \Im(z) \gg 1. \tag{2.11}$$

The conjugated symmetry should take place for the case $-\Im(z) \gg 1$. The structure at the right upper corner of Figure 1(b) is partially reproduced in the vicinity of the central part, above the real axis; the deviation is seen only at $y<1$. Let such behavior be the property of the analytic tetration F.

Assumption 2.

$$F(z) = L + \varepsilon(z) + o(\varepsilon(z)) \quad \text{at} \quad \Im(z)>0, \tag{2.12}$$

where $\varepsilon = \exp(Lz+r)$, and r is complex constant.

From Assumption 0 and Assumption 2 it follows that

$$F(z) = L^* + \varepsilon(z^*)^* + o(\varepsilon(z^*)^*) \quad \text{at} \quad \Im(z)<0. \tag{2.13}$$

In order to check that Assumption 2 is consistent with Figure 1(b), define functions F_+ and F_- as follows:

$$F_+(z) = L + \exp(Lz+\tilde{r}) \ , \tag{2.14}$$

$$F_-(z) = L^* + \exp(L^*z+\tilde{r}^*) \ . \tag{2.15}$$

Let

$$\mathrm{Fit}_4(z) = \begin{cases} F_+(z) & \text{for} \quad \Re(z)<-8 \ , \ \Im(Z)>0, \\ F_-(z) & \text{for} \quad \Re(z)<-8 \ , \ \Im(Z)<0, \\ \exp\bigl(\mathrm{Fit}_4(z-1)\bigr) & \text{for} \quad \Re(z)\ge\ 8. \end{cases} \tag{2.16}$$

Function Fit_4 is plotted in Figure 1(c) for

$$\tilde{r} = 1.07582 - 0.94664\ \mathrm{i} \tag{2.17}$$

in the range $|\Re(z)|\le 9$, $0.3<|3(z)|<2$. In this range, function $\mathrm{Fit}_4(z)$ looks very similar to $\mathrm{Fit}_3(z)$. I expect that $\tilde{r}$ approximates parameter r in equation (2.12), although I do not use this approximate value as the assumption, building up to the analytic extension of tetration.

The assumptions above leave to function F almost no freedom. $F(z)$ should have the cut at $x\le 2$; $F(n)=\mathrm{uxp}(n)$ at integer values of $n>-2$; $F(z)$ has logarithmic singularity at $z=-2$; $F(z)$ decays at $\pm\mathrm{i}\infty$ to its asymptotic values according to

(2.12), and it should quickly grow up in the positive direction of the real axis. In the vicinity of range $|y|<0.2x$, function $F(x+\mathrm{i}y)$ should show complicated, quasi-periodic and perhaps fractal behavior, similar to that of Fit_3 and Fit_4; fractal behavior is typical for iterated functions of complex variable [9].

3. Fits and asymptotic

Function Fit_4 by equation (2.16) has deep mathematical meaning. At $\Im(z)>0$ (upper part of Figure1(d)), it is just the shifted-argument approximation of the entire function

$$F_{\mathrm{entire}}(z)=\lim_{m\to\infty}\exp^m\Big(L+\exp(L(z-m))\Big)\ . \tag{3.1}$$

This function was described in the past century by Helmuth Kneser [11]; he used the notation $\mathcal{X}$ for the function such that

$$F_{\mathrm{entire}}(-z)=\mathcal{X}^{-1}(\mathrm{e}^{Lz})=\exp\Big(\mathcal{X}^{-1}\big(\exp(Lz+L)\big)\Big)\ . \tag{3.2}$$

Function F_{entire} satisfies equation (2.1), although it does not satisfy Assumption 0. Kneser analyzed the existence and uniqueness of this function and applied it for the construction of the function $\sqrt{\exp}$; such entire functions were under intensive research in the past century [12, 15, 16, 17], although ancient researchers did not have computer facilities for the efficient evaluation.

Due to Assumption 2, the combination of asymptotic (3.1) with fitting in the vicinity of the real axis allows one to approximate the function $F(z)$ at any complex z (except $z\le -2$):

$F(z)\approx\mathrm{Fit}_4(z)\approx F_{\mathrm{entire}}(z^*+r/L)^*$ can be used at $\Im(z)<-1$,
$F(z)\approx\mathrm{Fit}_3(z)$ can be used at $|\Im(z)|<2$), and
$F(z)\approx\mathrm{Fit}_4(z)\approx F_{\mathrm{entire}}(z+r/L)$ can be used at $\Im(z)>1$;

in the strips $1<|\Im(z)|<2$, both fits are valid, $\mathrm{Fit}_3(z)\approx\mathrm{Fit}_4(z)$.

The improvement of precision of the approximation can be achieved with numerical solution of equation (2.1) using the Cauchy integral.

4. Contour integral

In this section, the expression of the analytic tetration in terms of contour integral is suggested; this allows one to replace the functional equation (1.4) for function F with the integral equation for its values at the imaginary axis.

According to the assumption of the previous section, function F is analytic. In the range of analyticity, it can be expressed with the Cauchy contour integral [18, 19, 20, 21, 22, 23]:

$$F(z)=\frac{1}{2\pi\mathrm{i}}\oint_{\Omega}\frac{F(t)\ \mathrm{d}t}{t-z}, \tag{4.1}$$

where the contour Ω evolves the point z just once.

I apply the Cauchy formula (4.1) to express tetration $F(x+\mathrm{i}y)$ in the range $|x|\le 1$, $|y|\le A$, where A is the large positive parameter. Let the contour Ω consist of 4 parts:

A. integration along the line $\Re(t)=1$ from $t=1-\mathrm{i}A$ to $t=1+\mathrm{i}A$,
B. integration from point $t=1+\mathrm{i}A$ to $t=-1+\mathrm{i}A$, passing above point z,
C. integration along the line $\Re(t)=-1$ from $t=-1+\mathrm{i}A$ to $t=-1-\mathrm{i}A$,
D. integration from point $t=-1-\mathrm{i}A$ to $t=1-\mathrm{i}A$, passing below point z.

Such a contour has several advantages. Values at the imaginary axis are related to values at parts A and C through equation (2.1); as for the parts B and D, the integral can be estimated analytically, using the asymptotic values L and L^*. Then, tetration F can be expressed with four integrals:

$$F(z) = \frac{1}{2\pi}\int_{-A}^{A}\frac{F(1+\mathrm{i}p)\ \mathrm{d}p}{1+\mathrm{i}p-z} - \frac{1}{2\pi}\int_{-A}^{A}\frac{F(-1+\mathrm{i}p)\ \mathrm{d}p}{-1+\mathrm{i}p-z} - \frac{f_{\mathrm{up}}}{2\pi\mathrm{i}}\int_{-1+\mathrm{i}A}^{1+\mathrm{i}A}\frac{\mathrm{d}t}{t-z} + \frac{f_{\mathrm{down}}}{2\pi\mathrm{i}}\int_{-1-\mathrm{i}A}^{1-\mathrm{i}A}\frac{\mathrm{d}t}{t-z}\ , \tag{4.2}$$

where f_{up} is some intermediate value of function F at the upper part of the contour,

$$\min_{t\in\Omega_{\mathrm{B}}}\Re(F(t)) < \Re(f_{\mathrm{up}}) < \min_{t\in\Omega_{\mathrm{B}}}\Re(F(t)),\quad \min_{t\in\Omega_{\mathrm{B}}}\Im(F(t)) < \Im(f_{\mathrm{up}}) < \min_{t\in\Omega_{\mathrm{B}}}\Im(F(t))$$

and, similarly, f_{down} is the analogous intermediate value for Ω_{D}. F_{up} has no need to belong to the set of values of function F; at the contour Ω_B, there may exist no point z_{u} such that $F(z_{\mathrm{u}}) = f_{\mathrm{up}}$.

Using equations (1.4) and (2.1), the integrands in the first two integrals can be expressed in terms of the function F at the imaginary axis; the last two integrals can be simplified analytically.

The equation (4.2) is still exact. However, it becomes approximate when I substitute f_{up} and f_{down} with their asymptotic values, using the assumptions from the previous section. Such a substitution leads to the equation for the approximation F_A:

$$F_A(z) = \frac{1}{2\pi}\int_{-A}^{A}\frac{\exp\bigl(F_A(\mathrm{i}p)\bigr)\ \mathrm{d}p}{1+\mathrm{i}p-z} - \frac{1}{2\pi}\int_{-A}^{A}\frac{\ln\bigl(F_A(\mathrm{i}p)\bigr)\ \mathrm{d}p}{-1+\mathrm{i}p-z} + \mathcal{K}(z)\ , \tag{4.3}$$

where

$$\mathcal{K}(z) = L\left(\frac{1}{2} - \frac{1}{2\pi\mathrm{i}}\ln\frac{1-\mathrm{i}A+z}{1+\mathrm{i}A-z}\right) + L^*\left(\frac{1}{2} - \frac{1}{2\pi\mathrm{i}}\ln\frac{1-\mathrm{i}A-z}{1+\mathrm{i}A+z}\right)\ . \tag{4.4}$$

The placement of the cuts of the logarithms at the transition from equation (4.2) to equations (4.3) and (4.4) is not obvious; these cuts are shown in Figure 3. The figure represents the map of constant modulus and constant phase of the function $\mathcal{K}$ by equation (4.4). This function depends on a single real parameter A; for $A=3$, $A=5$ and $A=10$, the lines $|\mathcal{K}(z)| = \text{constant}$ and $\arg\bigl(\mathcal{K}(z)\bigr) = \text{constant}$ are shown in the complex z-plane. A thick dashed line indicates $\arg(\mathcal{K}) = \pm\pi$. Thick solid lines indicate the cuts of the logarithmic functions. Values of $\mathcal{K}$ in the shaded region are required for the evaluation of tetration; then, using equations (1.4) and (2.1), it can be extended to the range of Figure 1(c) and 1(d). Figure 3 shows also, that just neglecting $\mathcal{K}$ in equation (4.3) would lead to a poor approximation; huge values of A would be necessary to obtain good precision.

Consider the case $z = \mathrm{i}y$. This case is important, so I give a special name to the function $E(y) = F_A(\mathrm{i}y)$. At $z = \mathrm{i}y$, the equation for E can be written as follows:

$$E(y) = \frac{1}{2\pi}\int_{-A}^{A}\frac{\exp\bigl(E(p)\bigr)\mathrm{d}p}{1+\mathrm{i}p-\mathrm{i}y} - \frac{1}{2\pi}\int_{-A}^{A}\frac{\ln\bigl(E(p)\bigr)\mathrm{d}p}{-1+\mathrm{i}p-\mathrm{i}y} + \mathcal{K}(\mathrm{i}y). \tag{4.5}$$

From this equation, $E(y)$ should be found for the range $-A \le y \le A$. (The quadrature formula for the approximation may use values of the function at the tips of the interval of integration.) Then, from equation (1.4), the approximation F_A of the

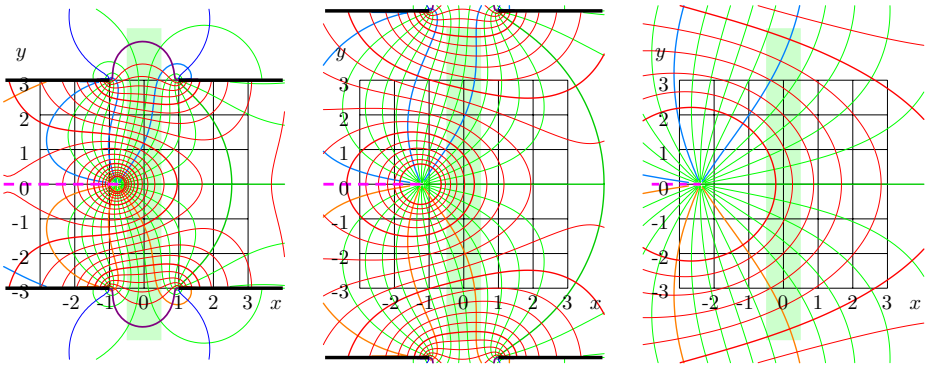

FIGURE 3. Behavior of the function $K=\mathcal{K}(x+\mathrm{i}y)$ by (4.4) at $A=3$ (left), 5 (central) and 10 (right). Levels $|\mathcal{K}|=1$, $\exp(-1)$, $\exp(-2)$, $\exp(-3)$, $\exp(-4)$ and $\arg(\mathcal{K})=0$, ±1, ±2, ±3 are shown with thick curves. Thick horizontal lines indicate the cuts of the logarithmic functions.

tetration $F(z)$ can be expressed for $|\Re(z)|<1$. For the precise evaluation, the value of z should be evolved by the contour, but should not approach it. For the evaluation, it is sufficient to work with $|\Re(z)|\le 0.5$ and then extend the approximation to the whole complex z-plane, except $z<-2$ with equation (1.4).

The solution E of equation (4.5) has no need to satisfy equality $E(0)=1$ exactly; the correction of the argument can be applied to the reconstructed tetration to satisfy condition (1.5).

In such a way, for reconstruction of the approximation F_A in the whole complex plane, it is sufficient to calculate it along the imaginary axis, or along any vertical line in the complex z-plane. The error of such an approximation comes from the replacement of the function at the upper and lower contour of integration to its asymptotic values. Due to the assumption about exponential decay of the tetration F to these asymptotic values, the number of correct decimal digits at the evaluation is proportional to parameter A. Another source of error arises at the approximation of integrals as finite sums for the numerical integration. While the contour does not get too close to the value z, the integration can be performed with high precision. One example of such an evaluation is described in the next section.

5. Numerical evaluation of tetration

For the numerical implementation, I replace the integrals in equation (4.5) with finite sums. The approximation with Gauss-Legendre quadrature formulas [6, 27] allow the good precision. Values $A=10$ and $N=100$ are sufficient to achieve the camera-ready quality of figures; at $A=24$ and $N=2048$, the precise check with 14 significant decimal digits can be performed.

For the computation, values of function E are stored in a mesh with nodes at y_n, for $n=0\dots N-1$; let E_n approximate $E(y_n)$, and let the integral of a function

f be approximated as follows:

$$\int_{-A}^{A} f(y)\ \mathrm{d}y \approx \sum_{n=0}^{N-1} W_n f(y_n). \tag{5.1}$$

Applying this rule to equation (4.5), I get the approximation

$$E_n = \frac{1}{2\pi} \sum_{m=0}^{N-1} W_m \left(\frac{\exp(E_m)}{1 + \mathrm{i}y_m - \mathrm{i}y_n} - \frac{\ln(E_m)}{-1 + \mathrm{i}y_m - \mathrm{i}y_n} \right) + \mathcal{K}(\mathrm{i}y_n). \tag{5.2}$$

Equation (5.2) gives a straightforward method for the iterational solution; just interpret the equality as operator of assignment. At the parallel assignment of the whole array E, the iterations may diverge; but they converge quickly, if the elements of the array E are updated one by one. Such an update is slow in high level languages such as Matlab, Mathematica and Maple; but it is fast at the implementation with C++. Several tens of iterations can be performed during a minute at a laptop class computer, giving the residual of the resulting approximation at the level of rounding errors.

Equation (4.5) looks similar to the equation of Fredholm of the second kind [26, 24, 25], but the kernel is nonlinear. The soluiton is stable, at least with a good initial approximation. For the convergence, the amplitude at the center of the grid should be of the order of unity; at positive values of y_n the phase should be nonnegative, and at the negative values of y_n, the phase should be nonpositive. An occasional appearance of zero in the solution gives an infinity in the evaluation of the logarithm and ruins the algorithm. In particular, the iterations do not converge with the conjugation of the function fit_2 by equation (1.9) as the initial distribution. For the initial condition

$$E_n = \begin{cases} L, & 3 < y_n, \\ \mathrm{Fit}_3(\mathrm{i}y_n), & -3 \le y_n \le 3, \\ L^*, & y_n < -3 \end{cases} \tag{5.3}$$

the algorithm converges to a smoothly-looking function after a few updates of each point of the mesh. The typical resulting function E is in Figure 4. For comparison, the initial condition is plotted with light strips. The real part of E is represented with a symmetric curve, and the imaginary part corresponds to the antisymmetric curve. Visually, I would not be able to distinguish these functions from scaled and shifted $1/\cosh$ and $\tanh$. At the zooming in, the defects (jumps) of the initial condition at $|y| = 3$ are seen, while the solution (thin lines) looks perfect. After a few tens of iterations, the precision of the resulting solution cannot be improved more due to the rounding errors.

The discrete analogy of equation (4.3) can be written as follows:

$$F_{A,N}(z) \quad = \frac{1}{2\pi} \sum_{n=0}^{N-1} \frac{\exp(E_n)\ W_n}{1 + \mathrm{i}y_n - z} \ - \ \frac{1}{2\pi} \sum_{n=0}^{N-1} \frac{\ln(E_n)\ W_n}{-1 + \mathrm{i}y_n - z} + \mathcal{K}(z)\ . \tag{5.4}$$

The function $F_{A,N}$ approximates F:

$$F(z) = \lim_{A\to\infty} \lim_{N\to\infty} F_{A,N}(z + x_1)\ ,\ |\Re(z)| < 1, \tag{5.5}$$

where x_1 is the solution of equation

$$F_{A,N}(x_1) = 1, \tag{5.6}$$

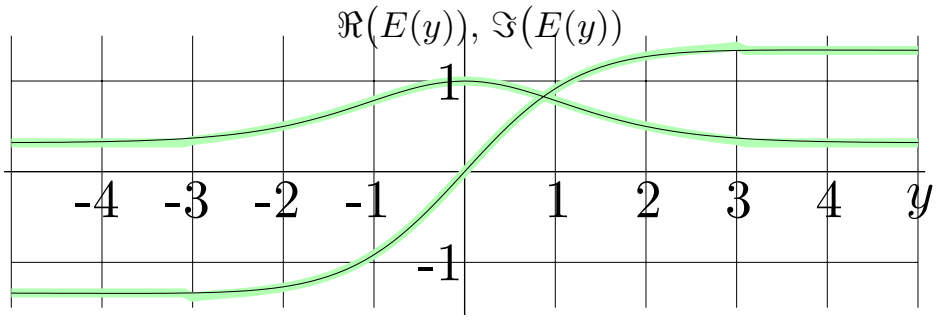

FIGURE 4. Initial condition of $E(y)$ corresponding to equation (5.3) versus y (thick lines) and the solution of equation (4.5) is calculated iterating equation (5.2) (thin lines). Real and imaginary parts are plotted.

which depends not only on A and N, but also on the initial condition, and on the mode of iterations. I use the automatic update of E_{N-1-n} each time when E_n is calculated, forcing the symmetry

$$E_{N-1-n} = E_n^* \,. \tag{5.7}$$

In this case, the displacement x_1 is always real. Typically, this correction is of order of one percent. Such a displacement of the argument should be applied each time when we have constructed a function satisfying equation (1.4) and want to get a function F which also satisfies condition (1.5).

The procedure above allows one to construct approximations of $F(z)$ within the strip $|\Re(z)|<1$. As the point z approaches the contour of integration, the approximations with finite sum become inaccurate. Therefore, equation (5.4) should be used for reconstruction of approximations of $F(z)$ at $|\Re(z)|\le 1/2$; values outside this range should be recovered using equation (2.1).

Function F evaluated in such a way is plotted in Figure 1(d). As it was mentioned, visually, it looks like a superposition of Figures 1(b) and 1(c).

At small values of $\varepsilon(z)$, oscillation of (2.14) is weak compared to the quick approach of the function to the asymptotic L; this oscillation is not seen in Figure 4. In order to reveal this oscillation, in Figure 5, the difference $F(z)-L$ is plotted in the same notation, as in Figure 1. In the upper-left corner of the figure, the lines of constant modulus and constant phase make an almost rectangular grid, typical for the exponential function. The figure makes an impression that the small ("linear") perturbation of the steady-state solution L of the equation of tetration comes from direction $-1.061+4.75\mathrm{i}$ and becomes strong in the vicinity of the real axis. The iteration of the exponential produces the quasi-periodic "garden" of self-similar "flowers" in the vicinity of the positive direction $y\approx 0.22x$. The conjugated wave of perturbation comes from the third quadrant of the complex plane. The condition (1.5) "synchronizes" these perturbations in such a way that the function $F(z)$ becomes zero at $z=-1$, causing the sequence of singularities at the negative part of the real axis and the cut at $z\le -2$.

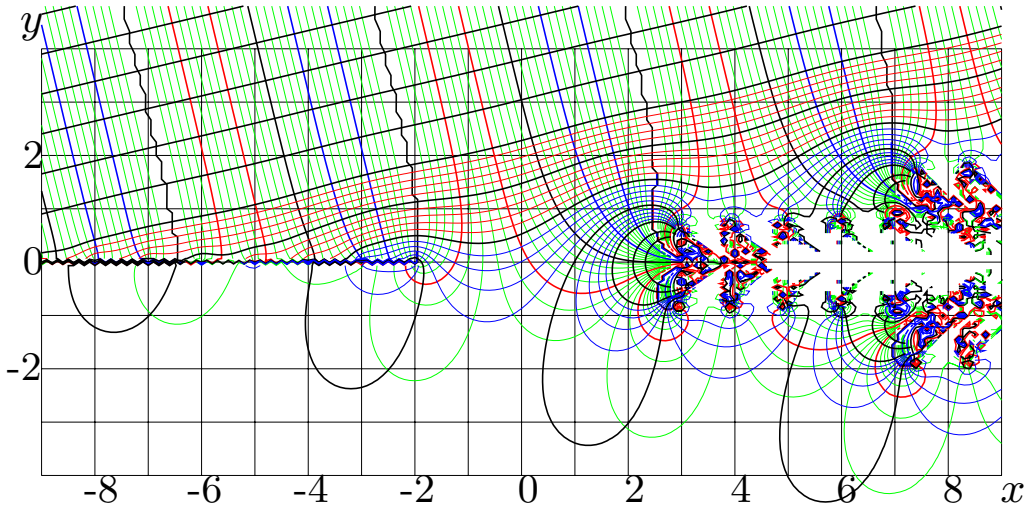

FIGURE 5. Lines of constant modulus and constant phase of $F(x+\mathrm{i}y)-L$ in the same notations as in Figure 1. Scratched lines indicate the jumps of phase.

Figures 1(d) and 4 and 5 confirm that the analytic tetration F with assumed properties can be approximated using integral equation (4.5). Visually, the plots of the resulting approximation satisfy the requirements formulated in Section 2.

6. Accuracy

The plots of tetration F raise the question of how precisely its analyticity can be checked. The precision of evaluation of function F with equation (5.5) depends on parameters A and N which are supposed to be large. In this section I show that at $A = 24$, using the Gauss-Legendre quadrature formula with $N = 2048$ points and double-precision arithmetic, the residual at the substitution of approximation (5.5) to the equation (1.4) becomes of order rounding errors.

Due to the smallness of the resulting parameter x_1 by equation (5.6), values of $F(z)$ at the imaginary axis are close to values of array E. For values of z, which are integer factors of 0.1 i, approximations for $F(z)$ are printed in Table 1. The representation (5.4) allows straightforward differentiation; so, I print the first derivative also. Similar data for the real axis are shown in Table 2. At the real axis, the function F is invertible; so, I print there also values of $t = F^{-1}(x)$ which is the solution of equation $F(t) = x$.

In order to estimate the precision of calculated values, consider the residual. From equation (2.1) it follows, that $F(-0.5 + \mathrm{i}y) = \ln\bigl(F(0.5 + \mathrm{i}y)\bigr)$. At real y, both $z = -0.5 + \mathrm{i}y$ and $z = 0.5 + \mathrm{i}y$ are inside the contour Ω of integration and within the range of approximation expected for the function $F_{A,N}(z)$. Functions $F_{A,N}(-0.5 + \mathrm{i}y)$ and $F_{A,N}(0.5 + \mathrm{i}y)$ are shown in the top part of figure 6. The bottom part of Figure 6 shows the real and imaginary parts of

$$\mathrm{residual}(y) = F_{A,N}(-0.5 + \mathrm{i}y) - \ln\bigl(F_{A,N}(0.5 + \mathrm{i}y)\bigr). \tag{6.1}$$

TABLE 1. Tetration F and its derivative at the imaginary axis

y	$F(\mathrm{i}y)$	$F'(\mathrm{i}y)$
∞	0.31813150520476 + 1.33723570143069 i	0.00000000000000 + 0.00000000000000 i
2.2	0.46205977590137 + 1.29516316398653 i	0.10524026273402 + 0.16943328263392 i
2.1	0.47984927595632 + 1.28360656694651 i	0.12642114268197 + 0.18649812732321 i
2.0	0.49938479980586 + 1.26976723502480 i	0.15095297930087 + 0.20432273436087 i
1.9	0.52073186937763 + 1.25329276909992 i	0.17918029261924 + 0.22268620786941 i
1.8	0.54393020954940 + 1.23379706941951 i	0.21142955072994 + 0.24129189880084 i
1.7	0.56898571838240 + 1.21086312875581 i	0.24798859588585 + 0.25975862529059 i
1.6	0.59586167470516 + 1.18404812970916 i	0.28908112588736 + 0.27761443401317 i
1.5	0.62446951205594 + 1.15289133555805 i	0.33483641789324 + 0.29429444323243 i
1.4	0.65465965324104 + 1.11692521645276 i	0.38525509140219 + 0.30914451353276 i
1.3	0.68621307873134 + 1.07569013479634 i	0.44017250164697 + 0.32143254761397 i
1.2	0.71883447558204 + 1.02875270845089 i	0.49922229471440 + 0.33036904052764 i
1.1	0.75214795374738 + 0.97572766747336 i	0.56180365001189 + 0.33513800375778 i
1.0	0.78569638858019 + 0.91630262108129 i	0.62705663243943 + 0.33493851305935 i
0.9	0.81894541361165 + 0.85026467624571 i	0.69385066719156 + 0.32903587645367 i
0.8	0.85129291145694 + 0.77752734034087 i	0.76079119151234 + 0.31681986197241 i
0.7	0.88208451053588 + 0.69815566451266 i	0.82624879777085 + 0.29786574159447 i
0.6	0.91063509163399 + 0.61238722872001 i	0.88841350542975 + 0.27199237376058 i
0.5	0.93625567282687 + 0.52064642918836 i	0.94537418225559 + 0.23931050362376 i
0.4	0.95828434050920 + 0.42354968973591 i	0.99521978881155 + 0.20025425056736 i
0.3	0.97611922542662 + 0.32189973245718 i	1.03615549420131 + 0.15558963085388 i
0.2	0.98925100004340 + 0.21666790754930 i	1.06662345026663 + 0.10639600379842 i
0.1	0.99729210719977 + 0.10896472393191 i	1.08541583925225 + 0.05401936304801 i
0.0	1.00000000000000 + 0.00000000000000 i	1.09176735125832 + 0.00000000000000 i

TABLE 2. Tetration F, its derivative, and its inverse at the real axis

x	$F_{A,N}(x+x_1)$	$F(x)$	$F'(x)$	$F^{-1}(x)$
-1.1	-0.00000001547015	-0.11279679776258	1.16819644635938	-1.67261575378528
-1.0	-0.00000000000000	-0.00000000000000	1.09176735125833	-1.63635835428603
-0.9	0.10626039927151	0.10626040042411	1.03653178245952	-1.59610183735171
-0.8	0.20785846728047	0.20785846728047	0.99791089741917	-1.55146594044381
-0.7	0.30629553437625	0.30629553437625	0.97291281085669	-1.50206743429127
-0.6	0.40282959178360	0.40282959178360	0.95959569174883	-1.44753575532149
-0.5	0.49856328794111	0.49856328794111	0.95675517789104	-1.38753447917073
-0.4	0.59450765927989	0.59450765927989	0.96374036331481	-1.32178907507892
-0.3	0.69163169510089	0.69163169510089	0.98034861830628	-1.25012048301963
-0.2	0.79090416202613	0.79090416202613	1.00677283707697	-1.17248262296575
-0.1	0.89333216876936	0.89333216876936	1.04358746497488	-1.08900005343708
0.0	1.00000000000000	1.00000000000000	1.09176735125832	-1.00000000000000
0.1	1.11211143309340	1.11211143309340	1.15273884603792	-0.90603157029014
0.2	1.23103892493161	1.23103892493161	1.22846715833643	-0.80786507256596
0.3	1.35838369631113	1.35838369631113	1.32158890019997	-0.70646669396340
0.4	1.49605193039935	1.49605193039935	1.43560498704373	-0.60294836953664
0.5	1.64635423375119	1.64635423375119	1.57515793778431	-0.49849837513117
0.6	1.81213853570187	1.81213853570186	1.74643105077407	-0.39430303318768
0.7	1.99697132461831	1.99697132461829	1.95772807888681	-0.29147201034755
0.8	2.20538955455274	2.20538955455274	2.22032629869699	-0.19097820800866
0.9	2.44325711324446	2.44325744833852	2.54975284679259	-0.09361896280296
1.0	0.59665094765656	2.71828182845904	2.96773135183036	0.00000000000000
1.1	0.00000003298313	3.04077200774189	3.50521601526880	0.08946084201600

For $A = 24$ and $N \geq 1024$, at the double-precision arithmetic, the typical values of this residual are of order of 10^{-14}. The residual characterizes the error of evaluation

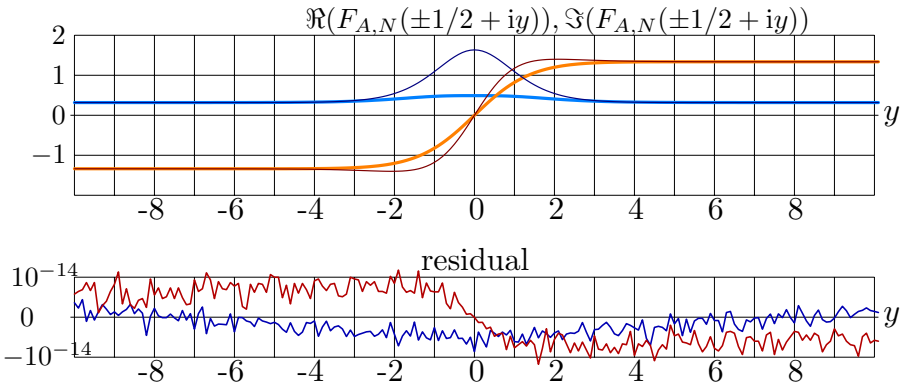

FIGURE 6. Real and imaginary parts of $F(\pm 1/2 + \mathrm{i}y)$ reconstructed at the array of $N = 2048$ nodes; function F reconstructed along the lines $z = 0.5 + \mathrm{i}y$ and $z = -0.5 + \mathrm{i}y$, top; residulal $F(-0.5+\mathrm{i}y) - \ln\bigl(F(0.5+\mathrm{i}y)\bigr)$, real and imaginary parts, bottom.

of function F, then the error of the values in Tables 1 and 2 is expected to be of order of unity in the last decimal digit of the mantissas.

The smooth trends in the lower part of Figure 6 are symmetric for the real part and anti-symmetric for the imaginary part; these trends should be attributed to the finiteness of the parameter A. (For smaller values $A = 20$, these trends were two orders of magnitude larger, and the deviation was at the level 10^{-12}.) The irregular structure in Figure 6 appears due to the rounding errors. For double-precision arithmetics, value $A = 24$ provides a reasonable compromise between the speed of evaluation and the precision: the error is due to replacement of f_{up} and f_{down} with the asymptotic values L and L^* and rounding errors give comparable contributions to the error of the resulting approximation.

A similar relation can be checked at the real axis; while the real part of the argument of the function $F_{A,N}$ does not exceed 0.8, the relation

$$F_{A,N}(x - .5) - \ln\bigl(F_{A,N}(x + .5)\bigr) \approx 0 \tag{6.2}$$

holds with 14 decimal digits. The left part of this equation scaled up with factor 10^{13} is plotted at the bottom of Figure 7.

The same data are used in Table 2. The zeroth column has a sense of the argument x; in this table, this argument runs real values from -1.1 to 1.1 . It is the same x that appears in Figure 7.

The first column represents the corresponding estimate $F_{A,N}(x + x_1)$, evaluated with equation (5.5) using value $x_1 = -0.00743143611046$. This value is specific for $A = 24$, $N = 2048$, initial condition (I used approximation Fit_3 in the central part of the initial distribution), on the order of updating values at the iterational solution, and even on maximal number of iterations, because the value at the center is not fixed; it drifts from iteration to iteration, decreasing for $\sim 10^{-13}$ per cycle of iterations. Indeed, 64 iterations were sufficient to make errors of the approximation comparable to the rounding errors at the double-precision arithmetic.

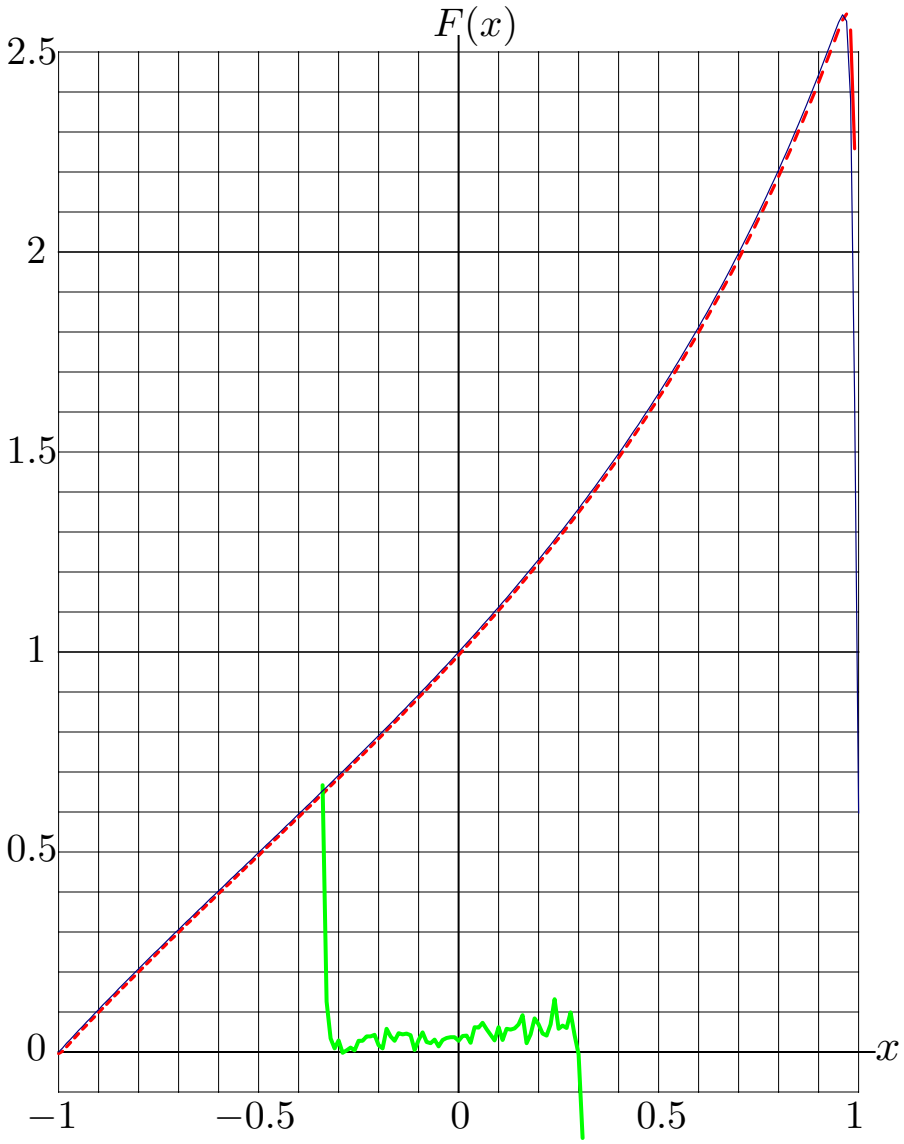

FIGURE 7. Bottom: left hand side of equation (6.2) scaled with factor 10^{13}. Central part: approximation $F_{A,N}(x)$ by equation (6.2) (dashed) and its correction $F_{A,N}(x+x_1)$ (solid).

However, the thirst column approximates the tetration F only in the central part of the table; at values $|x|>0.8$, the point x is too close to the contour of integration. Therefore, I offer the second column, where, at $|x|>0.5$, the value of tetration is estimated with equation (2.1); in the central part it coincides with the first column. This central part has length larger than unity, which confirms the high precision of the evaluation.

The third column is a derivative of tetration F. For the extension of the approximation to values $|x| > 0.5$, the following relations were used:

$$F'(z+1) = F'(z)\exp\bigl(F(z)\bigr)\ ,\ F'(z-1) = F'(z)/F(z). \tag{6.3}$$

The fourth column shows the inverse function; for each x, it contains value t such that $F(t) \approx x$; $|F(t) - x|$ is estimated to be of order of 10^{-14}.

In such a way, the first column of the table serves as confirmation of the procedure, the other three show behavior of tetration at the real axis.

I used the Gauss-Legendre quadrature with $N = 2048$ nodes in order to get a wide region with good approximation, $|x| < 0.8$, and to confirm that the equation $F(x+1) = \exp(F(x))$ holds with many decimal digits. At the evaluation of the function in the range $|x| \le 0.5$, the same precision can be obtained with $N \sim 1024$. The moderate number of nodes of the mesh is sufficient for the precise evaluation of the function F; this indicates the stability of the algorithm.

For the fast convergence, A should be of order of twice the number of correct decimal digits required in the estimate, and the initial condition for the array E should have values of order of unity at $y \approx 0$, of order of L at $y \gg 1$, and of the order of L^* at $-y \gg 1$. In particular, fast convergence takes place when Fit_3 is used for the central part of the initial distribution.

7. Inverse function

Tetration F can be used for calculation of functional fractal powers of exponential, and, in particular, $\sqrt{\exp}$ [11]. However, the inverse function F^{-1} is necessary for such an evaluation,

$$F(F^{-1}(z)) = z\ . \tag{7.1}$$

This function is shown in Figure 8. Function F^{-1} has singularities at fixed points L, L^* of the logarithm. These singularities are branch points that imply cuts. In order to simplify the comparison with Table 2, it is convenient to put the cuts along levels $\Re(F^{-1}(z)) = -2$. In this case, function F^{-1} has no singularities at the real axis. As $\Re(z) \to -\infty$, function $F^{-1}(z)$ approaches its asymptotic value -2 in the whole strip between cuts. In the positive direction of the real axis, function F^{-1} grows slowly (slower than any logarithm), whith corresponds to the rapid growth of tetration F.

8. Other tetrations

The results above refer to the specific function $F(x+\mathrm{i}y)$ that approaches fixed points of logarithm (2.4) at fixed real x and $y \to \pm\,\mathrm{i}\,\infty$. However, different requirements may lead to different tetrations. I compare them in this section.

We may require that the tetration is defined as a sequence of differentiable functions. An example of such a sequence is constructed below. Let

$$\begin{aligned} h_0(x) &= x, \\ h_n(x) &= x + \exp\bigl(h_{n-1}(x-1)\bigr) \quad \text{for integer } n > 0. \end{aligned} \tag{8.1}$$

The first elements of this sequence are plotted in the left hand side of Figure 9. The terms with h negative arguments give an exponentially small contribution; so, this sequence converges rapidly. Consider the limit

$$h_\infty(x) = \lim_{n\to\infty} h_n(x)\ . \tag{8.2}$$

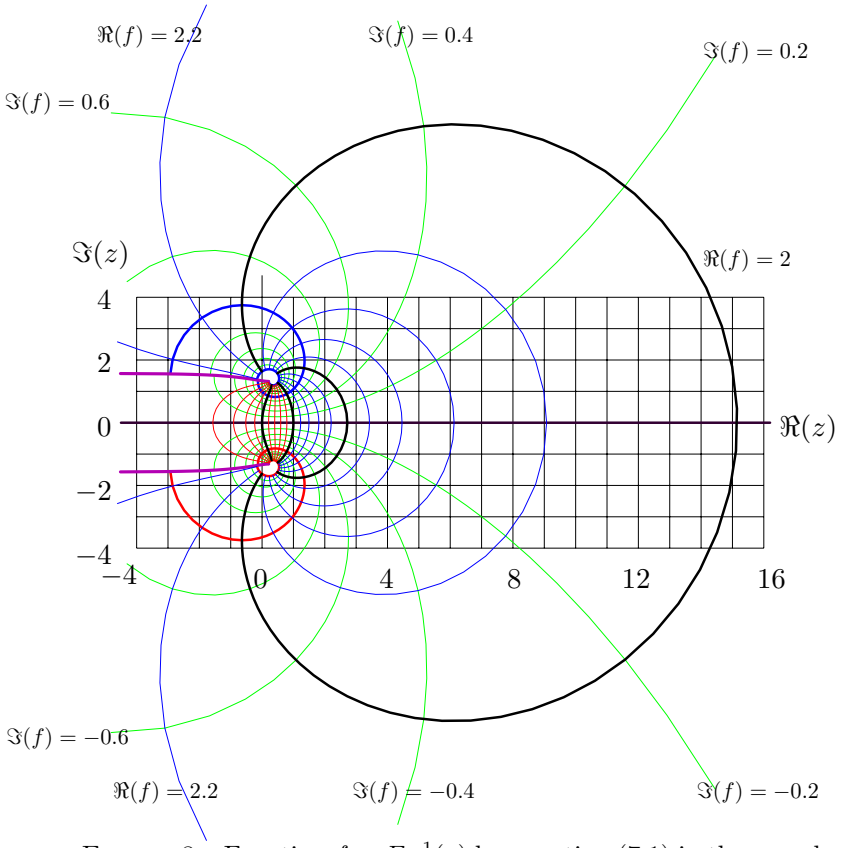

FIGURE 8. Function $f=F^{-1}(z)$ by equation (7.1) in the complex z-plane. Levels $\Re(f)=-2,-1,0,1,2$ and $\Im(f)=-2,-1,0,1,2$ (thick lines) and intermediate levels (thin lines).

The function h has rapid growth, similar to that of tetration. Their logarithms behave even more similarly. So, consider the functional sequence g such that

$$\begin{aligned} g_0(x) &= h_\infty(x)\,, \\ g_n(x) &= \ln\bigl(g_{n-1}(x+1)\bigr) \quad \text{for integer } n>0\,. \end{aligned} \tag{8.3}$$

For $x>-2$, this sequence also converges; the first few elements are shown in the right hand side of Figure 9. The limit

$$g_\infty(x)=\lim_{n\to\infty} g_n(x) \tag{8.4}$$

satisfies the equation (1.4); equation (1.5) is satisfied for function

$$F_{\rm g}(x)=g_\infty(x-x_0)\,, \tag{8.5}$$

where x_0 is the solution of equation

$$g_\infty(x_0)=1\,. \tag{8.6}$$

This equation can be solved numerically, giving value $x_0\approx 0.014322263393$. I compare such a tetration with the function F in Table 3.

At the real axis, in the range from minus unity to zero, every tetration $F(x)$ look similar to the function $1+x$. In Figure 10, I plot the difference between tetrations

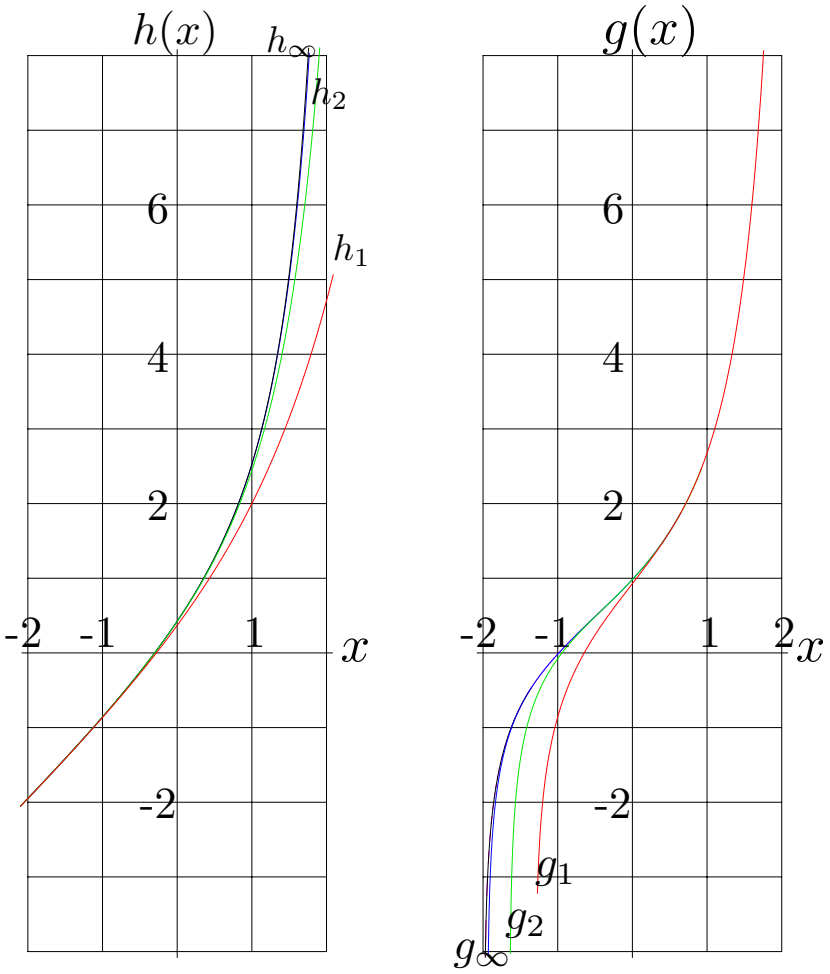

FIGURE 9. Functions h_1, h_2, h_∞ by equations (8.1) and (8.2); g_1, g_2, g_∞ by equations (8.3) and (8.4). In the graphics, h_3 almost overlaps h_∞ and g_3 almost coincides with g_∞, although the differences can be seen at the zooming in.

and this linear function. All the tetrations happen within a strip of width equal to one percent; the uxp function by (1.6) in this range just coincides with the abscissa axis, and all the tetrations deviate for less than one percent from uxp. Function $g_\infty(x - x_0) - (1+x)$ is shown with a thick line, and function $F(x) - (1+x)$ is plotted with a thin line. The difference $g_\infty(x-x_0) - F(x)$ is plotted in the lower part of Figure 10. At the same graphic, I also plot $\mathrm{Fit}_3(x) - F(x)$. In the range $-1 \le x \le 0$, the error of the approximation Fit_3 is of order of 10^{-4}.

The sinusoidal-like difference $g_\infty(x-x_0) - F(x)$ may mean, that there exist some analytic extension of g_∞, growing in the direction of imaginary axis with increment of order of 2π. In general, a lot of various analytic tetrations can be constructed

TABLE 3. Comparison of various tetrations

x	uxp(x)	$g_\infty(x-x_0)$	Fit$_3(x)$	$F(x)$
-1.1	-0.105360515658	-0.112273219465	-0.112743778423	-0.112796797763
-1.0	0.000000000000	-0.000000000001	0.000000000000	-0.000000000000
-0.9	0.100000000000	0.106179688230	0.106412412786	0.106260400424
-0.8	0.200000000000	0.208093402820	0.208104295564	0.207858467280
-0.7	0.300000000000	0.307095312397	0.306588453868	0.306295534376
-0.6	0.400000000000	0.404237363416	0.403131965155	0.402829591784
-0.5	0.500000000000	0.500408437490	0.498845079828	0.498563287941
-0.4	0.600000000000	0.596458714817	0.594745797295	0.594507659280
-0.3	0.700000000000	0.693307316434	0.691810291661	0.691631695101
-0.2	0.800000000000	0.792014962172	0.791015663894	0.790904162026
-0.1	0.900000000000	0.893800020573	0.893379533907	0.893332168769
0.0	1.000000000000	0.999999999999	1.000000000000	1.000000000000
0.1	1.105170918076	1.112021675762	1.112280500628	1.112111433093
0.2	1.221402758160	1.231328173701	1.231341586317	1.231038924932
0.3	1.349858807576	1.359470536292	1.358781651654	1.358383696311
0.4	1.491824697641	1.498159513017	1.496504365065	1.496051930399
0.5	1.648721270700	1.649394807818	1.646818228388	1.646354233751
0.6	1.822118800391	1.815677569929	1.812570126163	1.812138535702
0.7	2.013752707470	2.000320297393	1.997328008677	1.996971324618
0.8	2.225540928492	2.207840662685	2.205635473317	2.205389554553
0.9	2.459603111157	2.444400798181	2.443373176304	2.443257448339
1.0	2.718281828459	2.718281828457	2.718281828459	2.718281828459
1.1	3.019740552946	3.040499088409	3.041286147031	3.040772007742

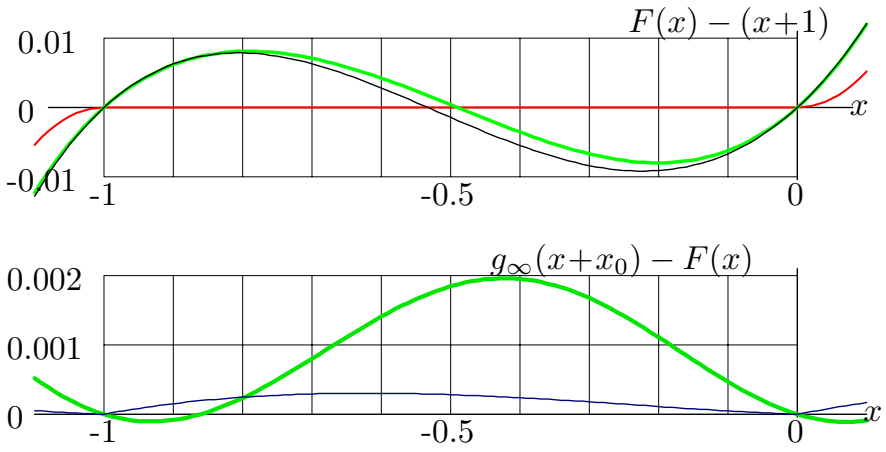

FIGURE 10. Comparison of various tetrations for the real argument. Upper graphic: Tetrations with substracted linear part: uxp$(x)-(x+1)$ (lies at the abscissa axis), $g_\infty(x+x_0)-(x+1)$ (thick curve), and $F(x)-(x+1)$ (thin curve). Lower graph: differences $g_\infty(x+x_0)-F(x)$ (thick line) and Fit$_3(x)-F(x)$ (thin line).

from function F in the form

$$G_\alpha(z) = F\left(z + \sum_{n=-\infty}^{\infty} \alpha_n \exp(2\pi i n z) \right) , \tag{8.7}$$

where coefficients are such that $\alpha_{-n} = \alpha_n^*$; they should decay at $n \to \infty$ fast enough to provide the convergence of the series. Such a G_α satisfies the initial equation in the title of the article, and $G_\alpha(0) = 1$ at $\alpha_0 = -\sum_{n\neq 0} \alpha_n$. In this sense, it can be considered as tetration, at least in the vicinity of the real axis. Outside the real axis, due to the exponential growth of some of terms, the argument of the "true" tetration F may get large negative values at relatively moderate values of z. Consider the imaging of the complex z-plane with function in the argument of F in (8.7). The image $Z(z)$ of a smooth contour in the range $|\Re(z)| < 1$ may cross the cut $Z < 2$; the resulting function G is not continuous. Roughly, at $|\Re(z)| < 1$, the range of analyticity of function $G(z)$ can be estimated with equation

$$|\Im(z)| \leq y_0 \sim \min_n \frac{d}{2\pi n \ln(|\alpha_n|)} , \tag{8.8}$$

where $d(z)$ is the distance from to the point z to the closest singularity of function F; for $\Re(z) > -2$ this distance $d(z) = |z + 2|$. The range of analyticity is only a strip along the real axis, even at small values of coefficients α. One has no need to evaluate function F in order to estimate the imaginary part of the singular points of the function G. The additional singularities and cuts of function G outside the real axis indicate that function F is the only tetration, analytic in the whole complex z-plane except for $z \leq -2$.

9. Fiber optics and the Abel equation

Pure mathematicians may skip this section; there are only speculations and no new formulas here. In this section I discuss the possible application of the algorithm used to calculate F above to the recovery of an analytic function from the recurrent equation.

Assume that one Manufacturer offers to some Scientist one piece of optical fiber of length, say, one meter, in exchange that the Scientist investigates and reports its nonlinear properties; but the Manufacturer does not allow the Scientist to cut the fiber to the smallest pieces. In the following, I treat this fiber as a single-dimensional homogeneous object. To be more specific, let the fiber be the optical amplifier with some transfer function H. I assume that the signal in the fiber is determined by its intensity. (This assumption tosses out many physical effects.) The laboratory of the Scientist is assumed to be well equipped, so, the Scientist can launch the signal of calibrated power and measure the transfer function H with as many decimal digits as he needs. Assume, he counts also with with an advanced software, which allows him to invert the transfer function and to extend it to the complex plane. In other words, the Scientist knows everything about the transfer function H, but the Scientist is not allowed to open the jacket of the fiber and to measure the power inside; he just believes the Manufacturer that the fiber is uniformly pumped. The signal power as the function of length of propagation is supposed to be continuous and analytic. How does one reconstruct this function in a long fiber, assuming, that at the coordinate zero, the signal power is just one watt?

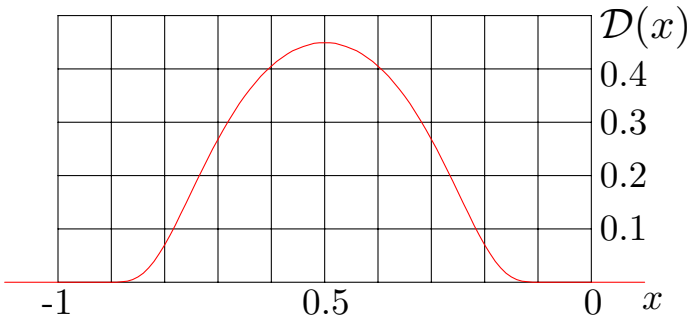

FIGURE 11. Graphic of the function $\mathcal{D}$ by equation (9.2).

Such a problem leads to the Abel equation [13, 14]

$$\varphi(z+1)=H\big(\varphi(z)\big); \tag{9.1}$$

$\varphi(x)$ may have a sense of the logarithm of the power of the signal in the fiber at coordinate x. In the case of $H=\exp$, this equation becomes (1.4), and F is one of its solutions. The Scientist knows the value of the function F at integer points, and wants to reconstruct the behavior in the whole real axis. In a similar way, if the Scientist has no idea about Gamma-function, he could "reconstruct" factorial values at the noninteger values of its argument using transfer function $H(z,f)=zf$; in this case, the transfer function has an additional argument, but it still leads to the recursive equation.

The simple approach could be just linear approximation. Choose one segment of unit length, approximate the solution with linear function at this segment and extend this approximation to the whole range, using equation (9.1). Such an approach is an analogy to the definition of ultraexponential $\mathrm{uxp}(x)$ by [3] at the segment $-1\le x\le 0$ and the extension to the real axis using equation (1.3).

The Scientist may expect, that function F is analytic, and reconstruct the solution of equation (9.1) with the desired behavior at $\pm i\infty$, just replacing exp and ln in the equations (4.5), (5.2), (5.4) to H and H^{-1}. However, after such a replacement, the straightforward iteration has no need to converge, then other methods of numerical solution of the system of nonlinear equations may be required to approximate array E. Knowledge of nonzero asymptotic values L and L^* in equation (4.4) seem to be important not only for the precision of the algorithm, but also for its convergence.

The requirement of analyticity of the reconstructed function is much stronger than just existence of all the derivatives along the real axis. Leaving from the real axis is important not only for efficiency of the evaluating algorithms, but also for the uniqueness of the solution. At the real axis, various differentiable functions may satisfy the equation (1.4), even if the additional requirement of the existence of all derivatives is applied. Let F be the solution; consider a new function $G(x)=F(x)+\alpha\mathcal{D}(x)$ defined at the range $0\le x\le 1$ and extended to the positive values of x using (1.4). Let α =constant and $\mathcal{D}(x)$ is function differentiable along the real axis (at least, $-1\le x\le 0$), which vanishes with all its derivatives at $x=-1$ and

$x=0$. Such a function can be

$$\mathcal{D}(x) = \begin{cases} \exp\bigl(-0.1/x^2 - 0.1/(x+1)^2\bigr), & (x+1)x \neq 0, \\ 0, & (x+1)x = 0. \end{cases} \tag{9.2}$$

The graphic of this function is shown in Figure 11. At the real axis, function $\mathcal{D}(x)$ has all the derivatives; in particular, in points $x = -1$ and $x = 0$; and all these derivatives are zero in these points. Then, the function G is also the solution, and has all its derivatives along the real axis.

The difficulties with reconstruction of real-differentiable and real-analytic functions seem to be typical for the analytic extension of a function to the real axis [1], and the extension to the complex plane seems to be essential for the robust evaluation at noninteger values of the argument.

10. Discussion

The precise numerical evaluation of analytic tetration, that remains limited at the imaginary axis, is aimed to catch any contradiction, following from the assumption of its existence. Such a contradiction could provide a hint to the generalization of the proof of the nonexistence by [3]. No such contradictions were detected. I conclude, that the analytic extensions or tetration exist, and one of them remains limited at $x \pm \mathrm{i}\infty$ for any real x.

The generalization of tetration can be expressed with equation (8.7); such tetration G may be analytic in the vicinity of the real axis. However, due to the exponential growth in the imaginary direction, the tetration G cannot satisfy Assumption 1, and the tetation F seems to be unique. The construction of the solution G growing up at $z \to \pm\mathrm{i}\infty$ and analytic in the upper half-plane is difficult, if at all, because the argument of the function F in (8.7) may have values which correspond to the cuts of the function F.

The method of recovery of an analytic function with required behavior at $\pm\mathrm{i}\infty$ may be useful also for the more general equation (9.1). In particular, at $H = \exp_a$, the equation becomes

$$F(x+1) = \exp(\ell F(x)) \; ; \tag{10.1}$$

where $\ell = \ln(a)$. At real values of ℓ of order of unity, this equation can be treated with similar contour integrals. At $\ell = \ln(2)$ such an extension applies to the fourth Askermann function [2], giving a plot [28], similar to Figure 1(d). The method may be useful in various applications and, in particular, in nonlinear fiber optics, while the behavior of some parameter along the fiber can be recovered from the transfer function of a piece of fiber. The practical application of such a recovery may be a matter for future research.

The function F^{-1}, approximated in the Table 2 for the real axis is only a special example. In general, the recursive exponential $\exp_a^z(t)$ may be treated as the function of 3 variables; then it may have 3 different kinds of inverse functions. The analysis of the analytic properties of such functions and the precise evaluation may be a matter for future research.

A similar approach can be used for the evaluation of elements of the functional sequence, determined with equations

$$F_3(z) = \exp(z)\ , \tag{10.2}$$

$$F_n(z+1) = F_{n-1}\big(F_n(z)\big) \text{ for integer } n\ , \tag{10.3}$$

$$F_n(0) = 1 \quad \text{for integer } n \geq 3\ , \tag{10.4}$$

and the condition that these functions remain analytic outside the real axis. Such a sequence may be a complex analogy of the Askermann functions [2]. Then, tetration F, considered above, appears as F_4; pentation appears as F_5, and so on. Tetration F_4 is already required for mathematics of computation, although it is not yet implemented as an upgrade of the floating point; pentation F_5 and the highest operations in this hierarchy may be needed in the future.

11. Conclusion

The numerical solution of equation (1.4) is consistent with requirements (1.5), (2.5) and (2.7) within 14 decimal digits. Such an agreement hints at the following theorem.

Theorem 0. *There exists the solution $F(z)$ of equation* (2.1)*, analytic in the whole complex z-plane except for $z \leq 2$, such that $F(z^*) = F(z)^*$, $F(1) = 0$, and, at $\Im(z) > 0$,*

$$F(z) = L + \mathcal{O}\big(\mathrm{e}^{Lz}\big)\ , \tag{11.1}$$

where $L \approx 0.31813150520476413 + 1.3372357014306895\ \mathrm{i}$ is the fixed point of the logarithm $\big(L = \ln(L)\big)$. There exists only one such solution of equation (2.1)*.*

The proof of such a theorem may be a matter for future research; I expect the function F with such properties is unique not only among solutions of equation (2.1), but also among solutions of equation (1.4).

The method of recovery of an analytic function with required properties at $\pm\mathrm{i}\infty$ from the transfer function may work also for the more general equation (9.1). The application for the analytic extension of $\exp_a^z(t)$ of different bases (in particular, $a=2$, see [28]) is straightforward. Similar methods may be used in physics and, in particular, in fiber optics.

Acknowledgements

The author is grateful to Henryk Trappmann, Andrew Robbins, Arthur Knoebel, H. Takuma, K. Ueda and J.-F. Bisson for important corrections and discussions. (Unfortunately, the envelope by A. Knoebel, sent in the spring of 2008 to ILS, was not delivered and I cannot yet correct the errors he perhaps indicates.) This work was partially supported by the 21st Century COE program, Japan.

References

1. P. Walker. Infinitely differentiable generalized logarithmic and exponential functions. Math. Comput., **57** (1991), 723-733. MR1094963 (92d:33049)
2. W. Ackermann. "Zum Hilbertschen Aufbau der reellen Zahlen". Mathematische Annalen **99**(1928), 118-133. MR1512441
3. M. H. Hooshmand. "Ultra power and ultra exponential functions". Integral Transforms and Special Functions **17** (8), 549-558 (2006). MR2246500 (2008b:26013)
4. N. Bromer. Superexponentiation. Mathematics Magazine, **60** No. 3 (1987), 169-174.

5. R. L. Goodstein. Transfinite Ordinals in Recursive Number Theory. J. of Symbolic Logic, **12**, (1947), pp. 123-129. MR0022537 (9:221d)
6. M. Abramovitz, I. Stegun. 1970. Table of special functions. National Bureau of Standards, NY.
7. I. S. Gradshteyn, I.M.Ryshik, 1980. Tables of Integrals, Series and Products. Academic, NY.
8. A. Knoebel. "Exponentials Reiterated." Amer. Math. Monthly **88** (1981), 235-252. MR610484 (82e:26004)
9. I. N. Baker, P.J. Rippon, "A Note on Complex Iteration." Amer. Math. Monthly **92** (1985), 501-504. MR801229 (86m:30024)
10. J. F. MacDonnell, Some critical points of the hyperpower function $x^{x^{\cdots^x}}$ International Journal of Mathematical Education, 1989, **20** no. 2, 297-305. MR994348 (90d:26003)
11. H. Kneser. "Reelle analytische Lösungen der Gleichung $\varphi(\varphi(x)) = \mathrm{e}^x$ und verwandter Funktionalgleichungen". Journal für die reine und angewandte Mathematik, **187** (1950), 56-67. MR0035385 (11:726e)
12. R. Isaacs. Iterates of fractional order. Canad. J. Math. **2** (1950), 409-416. MR0040560 (12:712c)
13. J. Laitochová. Group iteration for Abelõs functional equation. Nonlinear Analysis: Hybrid Systems **1**(2007), 95-102. MR2340265 (2008c:39032)
14. G. Belitskii, Yu. Lubish "The real-analytic solutions of the Abel functional equations". Studia Mathematica **134**(1999), 135-141. MR1688221 (2000f:39022)
15. J. Kobza, Iterative functional equation $x(x(t)) = f(t)$ with $f(t)$ piecewise linear. Journal of Computational and Applied Mathematics **115** (2000), 331-347. MR1747229 (2001g:39048)
16. M. Kuczma, On the functional equation. Ann. Polon. Math. **11** (1961) 161-175. MR0131681 (24:A1529)
17. J. C. Lillo, The functional equation $f^n(x) = g(x)$. Arkiv för Mat. **5** (1965), 357-361. MR0217468 (36:557)
18. G. Arfken, "Cauchy's Integral Formula". no. 6.4 in Mathematical Methods for Physicists, 3rd ed., Orlando, FL, Academic Press, pp. 371-376, 1985.
19. W. Kaplan, "Cauchy's Integral Formula". no. 9.9 in Advanced Calculus, 4th ed., Reading, MA, Addison-Wesley, pp. 598-599, 1991.
20. K. Knopp, "Cauchy's Integral Formulas". Ch. 5 in Theory of Functions Parts I and II, Two Volumes Bound as One, Part I. New York, Dover, pp. 61-66, 1996.
21. S. G. Krantz, "The Cauchy Integral Theorem and Formula". no. 2.3 in Handbook of Complex Variables. Boston, MA, Birkhäuser, pp. 26-29, 1999.
22. Morse, P. M. and Feshbach, H. Methods of Theoretical Physics, Part I. New York: McGraw-Hill, (1953), pp. 367-372. MR0059774 (15:583h)
23. F. S. Woods, "Cauchy's Theorem". no. 146 in Advanced Calculus: A Course Arranged with Special Reference to the Needs of Students of Applied Mathematics. Boston, MA, Ginn, pp. 352-353, 1926.
24. K. Atkinson. An Automatic Program for Linear Fredholm Integral Equations of the Second Kind. ACM Transactions on Mathematical Software **2** (1976), 1403-1413. MR0418489 (54:6528)
25. N. K. Albov. On a criterion for solvability of Fredholm equations. Math. USSR Sb. **55** (1986), 113-119. MR791320 (87c:47015)
26. J. Guy, B. Mangeot and A. Sales. Solutions for Fredholm equations through nonlinear iterative processes. J. Phys. A **17** (1983), 1403-1413. MR748773 (86e:65177)
27. W. H. Press, S. A. Teukolsky, W. T. Vetterling, B. P. Flannery. Numerical Recipes in C. Cambridge University Press. 1992. MR1201159 (93i:65001b)
28. D. Kouznetsov. Portrait of the analytic extension of the 4th Ackermann finction in the complex plane. http://en.citizendium.org/wiki/Image:Analytic4thAckermannFunction00.jpg

Institute for Laser Science, University of Electro-Communications, 1-5-1 Chofu-gaoka, Chofushi, Tokyo, 182-8585, Japan

E-mail address: dima@ils.uec.ac.jp